Phase transition of potassium atoms on silicene-(3 × 3)/Ag(111)

Cong Wang,[1] Huimin Wang,[2] Wenda Yao,[1] Sheng Meng,[2,3,*] Jinglan Qiu,[1,4,†] and Ying Liu[1,5]

[1]*College of Physics, Hebei Normal University, Shijiazhuang, Hebei 050024, China*

[2]*Beijing National Laboratory for Condensed Matter Physics and Institute of Physics, Chinese Academy of Sciences, Beijing 100190, China and School of Physical Sciences, University of Chinese Academy of Sciences, Beijing 100190, China*

[3]*Songshan Lake Materials Laboratory, Dongguan, Guangdong 523808, China*

[4]*Hebei Key Laboratory of Photophysics Research and Application, Hebei Normal University, Shijiazhuang, Hebei 050024, China*

[5]*Hebei Advanced Thin Films Laboratory, Hebei Normal University, Shijiazhuang 050024, Hebei, China*

(Received 15 April 2022; accepted 15 August 2022; published 29 August 2022)

Potassium (K) atoms are predicted to form a stable and ordered structure on silicene with high coverage. However, not much is known about the atomic structures of K atoms on silicene/Ag(111). Here, the adsorption of K atoms on monolayer silicene-(3 × 3)/Ag(111) has been studied by combined scanning tunneling microscopy and density functional theory (DFT) calculations. An intriguing structural phase transition from a dispersed phase to an ordered close-packed phase is found with the increasing of K density. DFT calculations reveal three metastable bridge adsorption sites for K on silicene-(3 × 3). K atoms show high mobilities in both the dispersed phase and around the vacancy defects or domain boundaries in the ordered phase, indicating a weak interaction between K and silicene-(3 × 3). A nearly V-shaped density of states has been found in scanning tunneling spectroscopy obtained on the ordered K/silicene-(3 × 3), which is suggested to be the Dirac signature of silicene-(3 × 3) by electronic band structure calculations. This study not only reveals the adsorption mechanism of K atoms on silicene, but also provides an approach to study the adsorption of alkali-metal atoms on other graphenelike two-dimensional materials.

DOI: 10.1103/PhysRevB.106.054111

I. INTRODUCTION

Silicene [1,2], a single sheet of Si atoms, is a graphenelike two-dimensional material that hosts massless Dirac fermions [3–5]. Unlike graphene, the low-buckled honeycomb structure due to the mixed sp^2-sp^3 hybridization between Si atoms makes silicene a highly chemically reactive surface [1,5]. The low-buckled structure also provides an additional degree of freedom for an electrically tunable band gap [6,7] and chemical functionalization in silicene. Although the structural and electronic functionalization of silicene by adsorption of foreign atoms or molecules has been widely studied theoretically [8–12], the experimental studies were mainly focused on the adsorption of oxygen [13,14] and hydrogen [15–17] thus far.

Alkali-metal (AM) atoms are highly reactive chemical species with a fairly simple hydrogenlike electronic configuration. Among the AM species, the adsorption of K atoms has been widely studied in graphite [18,19], graphene [20,21], and Si(111)-(7 × 7) [22,23] surfaces both theoretically and experimentally. Due to the low-buckled structure, AM atoms are predicted to have a much stronger binding to silicene than to graphene [8]. The large ratio of binding energy (E_b) to cohesive energy (E_c) makes it possible to realize stable and ordered structures of AM adatoms on silicene in experiment [8]. Li and K decorated silicenes were predicted to be promising host materials for hydrogen storage [24,25]. In addition, a sizable band gap may also be created in silicene by AM adsorption without degrading its high charge mobilities [9]. However, to date, not much is known about ordered AM structures on silicene. In 2013, Friedlein *et al.* studied the adsorption of K on silicene/ZrB_2(0001) by angle-resolved photoelectron spectroscopy (ARPES) and microspot low-energy electron diffraction (μ-LEED) [26]. They found a tunable silicene-substrate interaction and a structurally intact silicene layer upon K adsorption. Nevertheless, little attention has been paid to the basic adsorption mechanism of AM atoms on silicene. Specifically, the microscopic atomic structures of AM atoms on silicene are still elusive.

In this paper, we present scanning tunneling microscopy (STM) measurements for the structural phase transition of K atoms on silicene-(3 × 3) from a dispersed phase to an ordered close-packed K layer with the increasing of K coverages at 200 K. The dispersed phase appears as fuzzy noisy features in the STM image. A moderate tip pulse may desorb K atoms and restore intact silicene-(3 × 3). In the ordered K layer, three metastable bridge adsorption sites have been calculated. K atoms easily hop among these three sites around defects and boundaries. Scanning tunneling spectroscopy (STS) shows a nearly V-shaped density of states around the Fermi level (E_F) on the ordered K/silicene-(3 × 3), which is suggested to be an observation of the Dirac signature of silicene-(3 × 3). Our work paves the way for further investigation of other AM atoms on silicene and other two-dimensional graphenelike materials.

*smeng@iphy.ac.cn
†jlqiu@hebtu.edu.cn

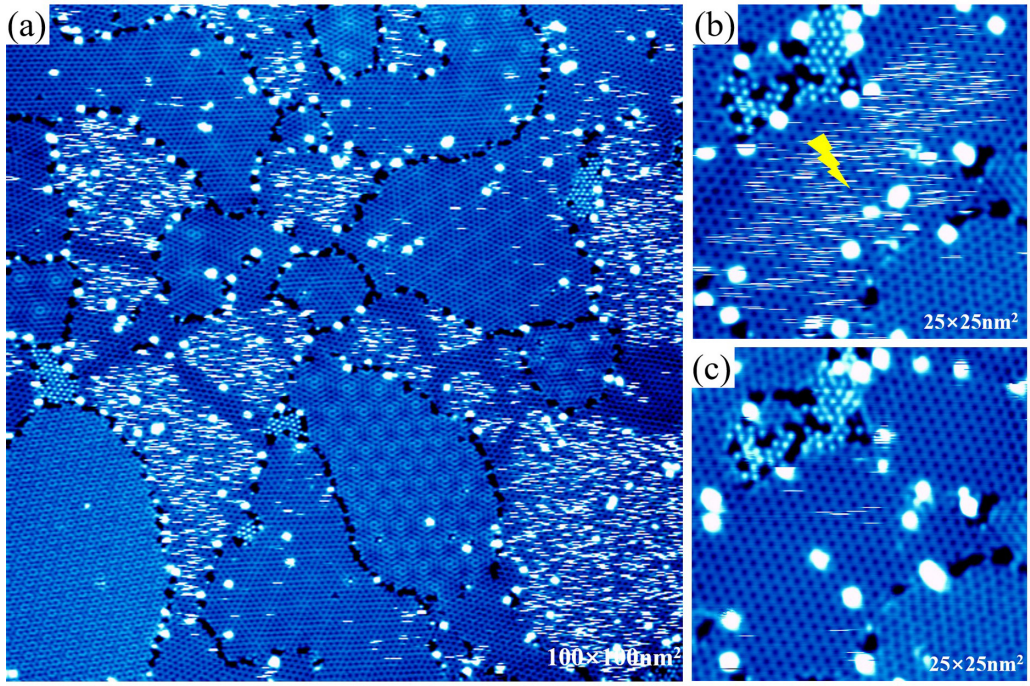

FIG. 1. K atoms form a dispersed phase on silicene/Ag(111) at a small amount (about 0.04 ML). (a) K atoms adsorb on multiphase silicene and form fuzzy and noisy features (the brightest features) with a selective adsorption tendency. (b) A controlled tip pulse (+6.5 V, 100 ms) on K/silicene. The yellow feature marks the tip position when doing the pulse. (c) The same area as (b). After the tip pulse, K atoms desorb from the surface and intact silicene-(3×3) recovers.

II. EXPERIMENTS AND CALCULATIONS

The experiments were performed in an ultrahigh vacuum (UHV) low-temperature STM and molecular beam epitaxy (MBE) combined system (CreaTec) with a base pressure of 6×10^{-11} mbar. A single-crystal Ag(111) surface was cleaned *in situ* by repeated cycles of Ar^+ sputtering followed by annealing to about 950 K. Silicon was deposited onto the Ag(111) substrate, which was held at 570 K, by resistively heating a small piece of silicon wafer at a temperature of about 1300 K. K atoms were evaporated from a well-degassed commercial thermal getter source (SAES) for several seconds to a few minutes by passing a direct current of 5.8 A through it. During K deposition, silicene was cooled down to about 200 K by continuous liquid nitrogen flow. K coverage is roughly defined by the ratio of the surface area covered by K atoms to the whole area of the surface scanned by STM. After K deposition, the sample was immediately transferred to the STM stage for data collections at 77 K with an etched tungsten tip. The bias voltage was defined as the sample bias with respect to the tip. Processing of the STM images was carried out with WSxM and SPIP software. The STS curves were acquired using the lock-in amplifier module integrated in the Nanonis controller by applying a small sinusoidal modulation to the sample bias voltage (typically 10 mV at 676 Hz). Calibration of the STS spectra was achieved on a clean Ag(111) surface.

The calculations were performed using density functional theory (DFT) as implemented in the Vienna *ab initio* simulation package (VASP) [27] with the Perdew-Burke-Ernzerhof (PBE) exchange-correlation functional [28] and projector-augmented wave (PAW) pseudopotentials. The plane-wave basis set with an energy cutoff at 350 eV was applied. In the calculation, the (3×3) supercells of silicon film on the seven-layer (4×4) Ag(111) surface with the lattice constant of 11.56 Å were chosen. The vacuum region of >15 Å in the surface normal direction is sufficiently large to eliminate artificial interactions between periodic images. All the structures were fully relaxed with the bottom four layers of Ag atoms fixed. The Brillouin zone is sampled by a $5 \times 5 \times 1$ Monkhorst-Pack k mesh. Geometry optimization was carried out until the residual force on each atom was less than 0.04 eV/Å.

III. RESULTS AND DISCUSSIONS

A. Dispersed phase and selective adsorption

The monolayer silicene on the Ag(111) substrate exhibits various phases, including (3×3) [refer to the Si-(1×1) lattice], $(\sqrt{13} \times \sqrt{13})R13.9^\circ$ and $(2\sqrt{3} \times 2\sqrt{3})R30^\circ$ [refer to the Ag-(1×1) lattice] [29–32]. Figure 1(a) shows an overview STM image of about 0.04 monolayer (ML) of K atoms on multiphase silicene (here 1 ML represents a close-packed K layer with the atomic density of 5.4×10^{14} cm^{-2}). The overall topography of multiphase silicene remains unchanged upon K adsorption. However, some specific domains are covered by fuzzy and noisy features. The amount of fuzzy features rises with the increasing of K density. Excluding the possibilities of contaminants and electronic or mechanical noises, the fuzzy features are indicative of moving K atoms on silicene. It is the so-called "dispersed phase" in K/graphite at low coverages [33]. For AM atoms (Na, K, Cs,

but not Li) on Si(111)-(7 × 7) at room temperature [22,34], a two-dimensional (2D) gas phase also appears at initial coverage, like the dispersed phase. In K/graphite, the dispersed phase is believed to result from electrostatic repulsion between the partially ionized K atoms after charge transfer to graphite [33]. Charge transfer also has been predicted from K atoms to silicene, resulting in positively charged K [8]. Therefore, we suggest a similar repulsive interaction between the positively charged K atoms on silicene in the dispersed phase.

Interestingly, Fig. 1(a) shows an obvious site selective adsorption tendency for K on silicene in the dispersed phase. The bright fuzzy noisy features show an inhomogeneous distribution, indicating that K atoms do not adsorb on all silicene phases. Now the question is which silicene phase is it under the fuzzy features? In an occasional tip poking process, we found that K atoms were removed from the surface under a STM tip pulse without destroying the underlying silicene. Inspired by this, we applied a controlled tip pulse (+6.5 V, 100 ms) in the middle of Fig. 1(b). After the tip pulse [Fig. 1(c)], the fuzzy features disappear and a clean silicene-(3 × 3) is completely recovered. K atoms adsorb preferentially on silicene-(3 × 3) in low coverages. As silicene-(3 × 3) is the simplest and most well understood one among the various silicene phases on Ag(111), we choose this phase as a model system for K adsorption.

B. Ordered close-packed phase

Figure 2(a) presents a typical STM image of clean silicene-(3 × 3). A continuous silicene-(3 × 3) usually contains both the stable (3 × 3)-α phase and metastable (3 × 3)-β phase [15,35]. The inset image shows the high-resolution STM image of the (3 × 3)-α and -β phases. Due to the different buckling configurations of the Si atoms, the two phases are different in appearance. As illustrated in Fig. 2(a), the large bright areas correspond to the (3 × 3)-α phase and the dark boundaries surrounding the α phase correspond to the (3 × 3)-β phase. The contrast between the (3 × 3)-α and -β phases is characteristic of silicene-(3 × 3), which helps us pick this phase out easily from the STM image of multiphase silicene.

Above 0.04 ML, with the increasing of K density, the amount of fuzzy features decreases, while more and more localized single K atoms appear, gather together, and finally assemble into an ordered close-packed K layer on silicene-(3 × 3) in the coverage of about 0.17 ML, as exemplified in Figs. 2(b)–2(e). Some vacancy defects characterized by "missing atom" structure can be observed in Fig. 2(c). The fast Fourier transform (FFT) image in the inset of Fig. 2(b) confirms the hexagonal patterns related to the ordered K layer. The line profile in Fig. 2(f) shows a similar lattice constant (1.14 nm) of ordered K layer with silicene-(3 × 3), suggesting that the K layer also exhibits a (3 × 3) period [refer to Si-(1 × 1) lattice]. Therefore, K atoms undergo a structural phase transition on silicene-(3 × 3) from a dispersed phase to an ordered close-packed K layer with the increasing of K coverages.

Besides the ordered hexagonal protrusions shown in Fig. 2(e), two different types of domain boundaries can be clearly seen in Fig. 2(b). The first type appears as connected dark, closed honeycomblike structures, which divide the ordered K protrusions into different domains. We call it the "interdomain boundary" and mark it with DB_{inter}. A close examination of Fig. 2(a) [clean silicene-(3 × 3)] and Fig. 2(b) [K/silicene-(3 × 3)] shows that DB_{inter} shares a similar connected honeycomblike shape, location, and dark character with the silicene-(3 × 3)-β phase. Indeed, when we increase K coverages, we found K atoms always adsorb on the silicene-(3 × 3)-α phase first and then the (3 × 3)-β phase, no matter whether in the dispersed phase or ordered phase. Since it is difficult to control the coverage precisely to get both silicene-(3 × 3)-α and (3 × 3)-β phases perfectly covered by K atoms, the structure of K on the (3 × 3)-β phase is usually more defective [red arrows in Fig. 2(b)]. The other type of domain boundary lies inside the ordered K domains. In Fig. 2(b), we find that K atoms are not perfectly long-range ordered; instead, they form parallel line defects in some places [black arrows in Fig. 2(b)]. Figure 2(d) shows an example of the line defects and the unit cells of the two adjacent areas. It is obvious that the two sets of unit cells do not overlap after translation, indicating that K atoms occupy different adsorption sites. Since this type of boundary always appears inside K domains, we call it the "intradomain boundary" and mark it with DB_{intra}. Around the DB_{intra}, some vacancy defects and fuzzy features can also be observed.

TABLE I. The adsorption energies (E_{ads}) of potassium atoms' adsorption at the three bridge sites (B_1, B_2, and B_3) on silicene-(3 × 3)/Ag(111). The adsorption energy differences (ΔE_{ads}) of K atoms in between the B_1, B_2, and B_3 adsorption sites and the B_2 adsorption site.

Structure	E_{ads}(eV)	ΔE_{ads}(meV)
K/silicene-(3 × 3)/Ag(111)-B_1	–2.274	0.27
K/silicene-(3 × 3)/Ag(111)-B_2	–2.274	0.00
K/silicene-(3 × 3)/Ag(111)-B_3	–2.272	2.25

According to our STM observations, the lattice constant of the ordered K layer is the same as the silicene-(3 × 3)-α phase. Therefore, it is natural to expect an adsorption picture of one K atom in one (3 × 3)-α unit cell. Our DFT calculations show that K atoms bind most strongly to the bridge sites (B) above the Si-Si bond, agreeing well with the results of Lin *et al.* [8]. For the sake of completeness, we have also computed the "hollow" and "on-top" sites; they all show higher energy than the bridge sites and thus can be definitively ruled out. Our calculations suggest three possible bridge adsorption sites. To explain it more clearly, let us focus on one silicene-(3 × 3)-α unit cell that is marked with a white rhombus in Fig. 3(a). Taking into account the substrate Ag atoms, there are 27 bridge sites in one unit cell. However, only three bridge sites where Si-Si bonds sit right on top of Ag atoms [marked with B_1, B_2, and B_3 in Fig. 3(a)] are calculated to be the most stable adsorption sites. Table I shows the adsorption energies of K atoms on the B_1, B_2, and B_3 sites, which are –2.274, –2.274, and –2.272 eV, respectively. Obviously, the adsorption energy difference among these three bridge adsorption sites is only about 2.3 meV (nearly zero), which indicates a

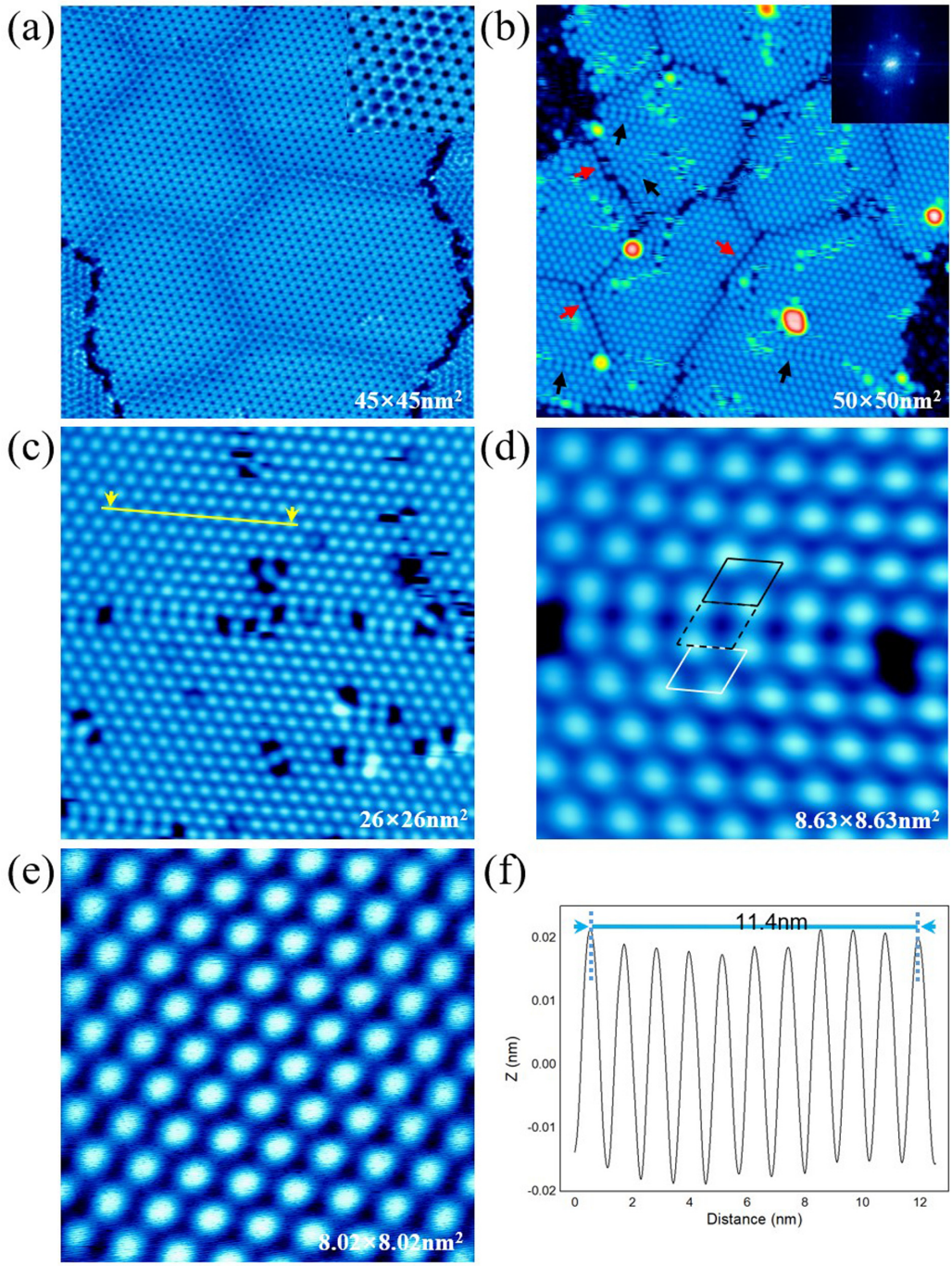

FIG. 2. K atoms form ordered a close-packed K layer on silicene-(3 × 3) in a coverage of about 0.17 ML. (a) The constant current STM image of clean silicene-(3 × 3)-α and -β phases. The inset image shows the atomic resolution. (b) The ordered close-packed K layer on silicene-(3 × 3). The red arrows represent the interdomain boundary (DB_{inter}). The black arrows represent the intradomain boundary (DB_{intra}). The inset image shows the fast Fourier transformation (FFT) of (b). (c) Enlargement image of close-packed K film shows some vacancy defects and DB_{intra}. (d) The STM image of a DB_{intra}. The black and white rhombuses correspond to the unit cells of K protrusions above and below the DB_{intra}, respectively. A translation of the black unit cell (dotted line) does not match the white one. (e) The STM image of a perfect area of the K layer. (f) The z profile along the yellow line in (c).

similar thermodynamic possibility for K atom adsorption on these three bridge sites.

Figures 3(b)–3(d) show the relaxed structures and simulated STM images of K atom adsorption on B_1, B_2, and B_3, respectively. In the unit cells of these structural models, one K atom (purple) corresponds to 18 Si atoms (red and yellow), or 16 Ag atoms (blue). Around each K atom, there are the four highest-buckling Si atoms marked with red balls. These four Si atoms make the middle bridge site a "potential well" that traps one K atom in it. The simulated STM images in the inset of Figs. 3(b)–3(d) show ordered hexagonal structure, in agreement with our STM observations. However, the protrusions in

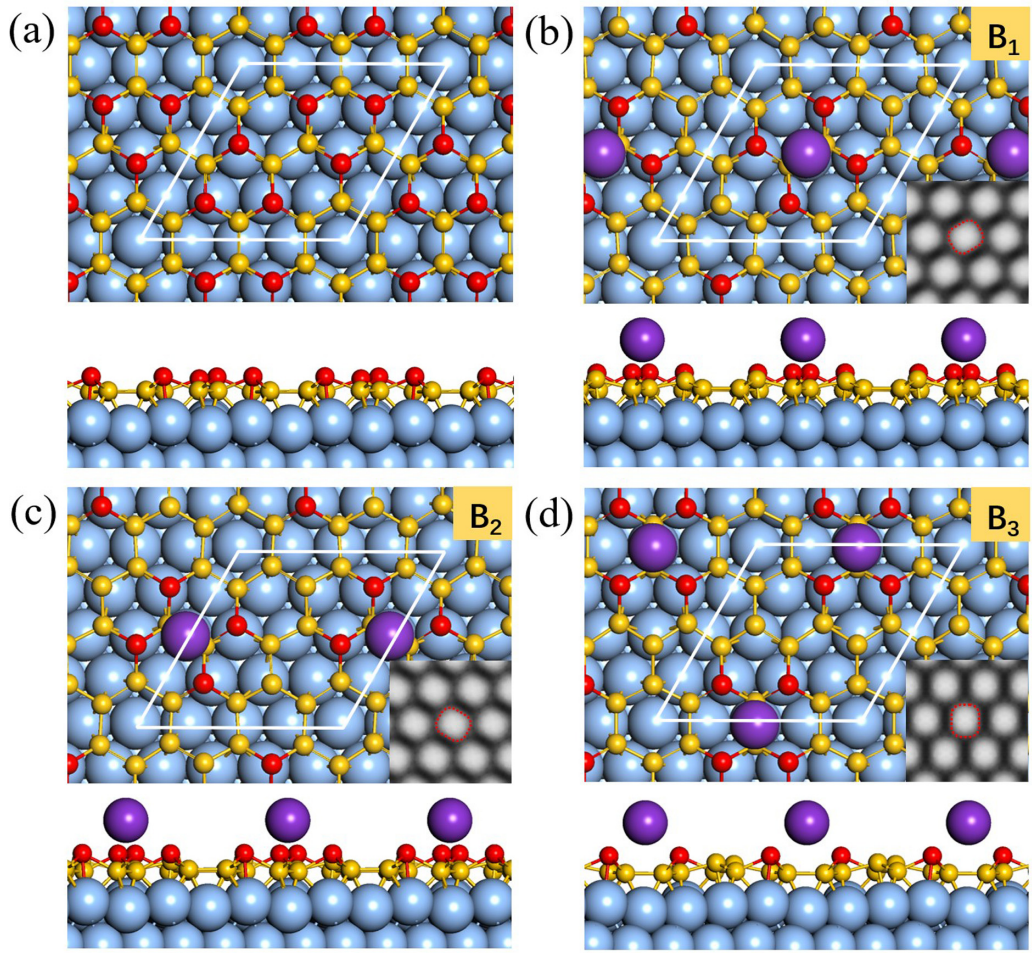

FIG. 3. Calculated structures and simulated STM images of K on the silicene-(3×3)-α phase. (a) The structural model of the silicene-(3×3)-α phase. The white rhombus corresponds to a unit cell. The red spheres are the highest-buckled Si atoms. The yellow spheres represent the lower-buckled Si atoms. The blue spheres are Ag atoms. (b–d) The calculated structural models of K on three bridge sites of silicene (marked by B_1, B_2, and B_3, respectively). The purple spheres represent K atoms. The inset images on the lower right of (b–d) are simulated STM images.

these simulated images are not perfectly spherical structures; instead, they are distorted along specific orientations, depending on the adsorption sites.

It is worth noticing in the high-resolution STM image [Fig. 2(e)] that the bright K protrusions are also not perfectly spherical. They show distorted shapes along a specific orientation and appear as ellipsoids. At first glance, the distortion of the K protrusions is naturally explained by artifacts in STM caused by the tip effect, thermal drift or piezocreep. Since piezocreep usually occurs at the beginning of the scanning, only the first few pixels of the image will be affected, and it will not result in a homogeneous distortion in the whole image like Fig. 2(e). Therefore, the origin of piezocreep could be excluded. The tip effect and thermal drift can also be excluded by our STM observation in Fig. 4(a). In Fig. 4(a), three DB_{intra} join together with 60° between each other and then divide the protrusions into three areas. Obviously, the protrusions in the three areas are distorted too. However, they are not distorted in the same orientation, but in three different orientations with 60° between each other. This observation confirms that the distorted K protrusions in the STM image are real structures, not tip or thermal drift related artifacts. We suppose the distortion of the K protrusions may result from intrinsic geometric or electronic structures in K/silicene.

To explain the distortion of the K protrusions, we draw the structural model of Fig. 4(a) in Fig. 4(b) based on the three bridge adsorption sites calculated before. The three ordered K domains are formed by the adsorption of K atoms on B_1, B_2, and B_3, respectively, resulting in three DB_{intra} that marked by the yellow lines. In Fig. 4(b), the two sets of unit cells (black and white rhombuses) are shifted along the Ag-Ag bond direction by a distance of double the Ag-(1×1) lattice, agreeing with Fig. 2(d). This observation provides additional evidence for the three bridge adsorption sites. To further reveal the origin of distorted K protrusions, we extend the considerations from only K atoms to K and Si atoms. According to the K/silicene structural models shown in Figs. 3(b)–3(d), four silicon atoms that are marked by red balls around each K atom show the highest buckling after K adsorption. Since the brightness of protrusions in the STM image reflect both geometrical height and electronic states, we suppose the four Si atoms might contribute electronic states in the STM image. To confirm this, we perform charge density calculations. Figures 4(c) and 4(d) show charge

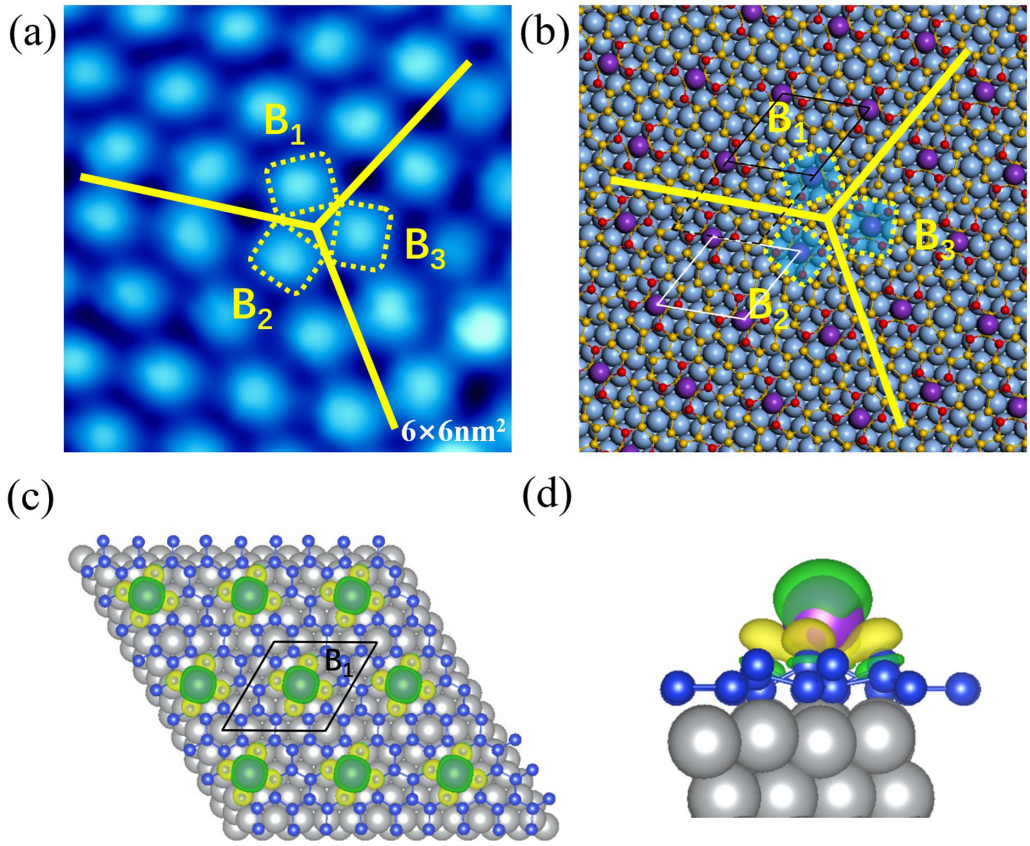

FIG. 4. The distortion of K protrusions. (a) The high-resolution STM image of the intersection of three intradomain boundaries (DB_{intra}). K protrusions show different distorted orientations in different domains. The yellow lines represent the locations of three intradomain boundaries (DB_{intra}). (b) The structural model of (a) based on the three bridge adsorption sites, which agrees well with the STM image. The slight distortion of each K atom (purple spheres) can be explained by the cocontribution charge densities of the K atom and the four high-buckling Si atoms (red spheres) around it. (c,d) The top and side views of the charge density difference calculated for the adsorption of K atoms on B_1. The yellow color represents the increasing of charge density on Si atoms, and the green color represents the decreasing of charge density on K atoms.

transfer from the middle K atom to the four Si atoms. As a result, the charges that localized in the middle K atom and the four Si atoms both contribute to the STM image, resulting in ellipsoidal protrusions [8,10]. A similar phenomenon has also been reported in the Na/Si(111)-(7 × 7) system, where Na atoms transfer charges to the nearest Si adatom, making it brighter in the filled state STM image [34].

More evidence to support the three metastable bridge adsorption sites is the hopping of K atoms around defects and boundaries. In Fig. 1, we have known that K atoms show high mobility on silicene in the dispersed phase. With the increasing of K density, K atoms continue to compress until reaching a critical coverage that a close-packed structure nucleates. Inside the perfectly ordered close-packed domain, K protrusions are stable enough. However, around the vacancy defects and domain boundaries, K atoms still present high mobility. In the sequential STM scans shown in Figs. 5(a)–5(d), we observe the changes of DB_{intra} and vacancy defects. According to the three bridge adsorption sites discussed above, we achieve the structural models shown in Figs. 5(e)–5(h), which correspond to the STM images in the inset. The structural models and inset STM images in Figs. 5(e) and 5(f) show that one K atom jumps from B_2 to B_3, resulting in the movement of the single-vacancy defect, which is marked by a white rectangle in the upper part of Figs. 5(a) and 5(b). For the DB_{intra} marked by a yellow rectangle shown in Figs. 5(g) and 5(h) and the lower part of Figs. 5(a) and 5(b), one K atom (locates on B_2 first) jumps to the nearest vacancy defect (B_3, marked by yellow arrows), and then drives its nearest K atoms to jump one by one along the boundary, resulting in the shifting of the DB_{intra} from left to right and leaving a single-vacancy defect on top (marked by red arrows). Over a sustained period of time, the DB_{intra} and vacancy defects in the area marked by a yellow rectangle in Fig. 5(c) disappear and become a perfectly ordered K layer [Fig. 5(d)]. These phenomena indicate that, around vacancy defects or domain boundaries, K atoms are able to diffuse among the B_1, B_2, and B_3 adsorption sites. As these events happen during normal sequential scanning at liquid nitrogen temperature, some external disturbance from the tip, thermal drift, or the electric field between tip and sample may trigger the diffusion. Since the rate of K atom hopping between sites depends on the energy barriers along the diffusion path, more future calculations are still needed to reveal the diffusion mechanism. When K/silicene is annealed to 660 K, nearly all of the K atoms desorb from the surface and the initial intact silicene is restored. The adsorption of K atoms on silicene is reversible, like hydrogenation [15].

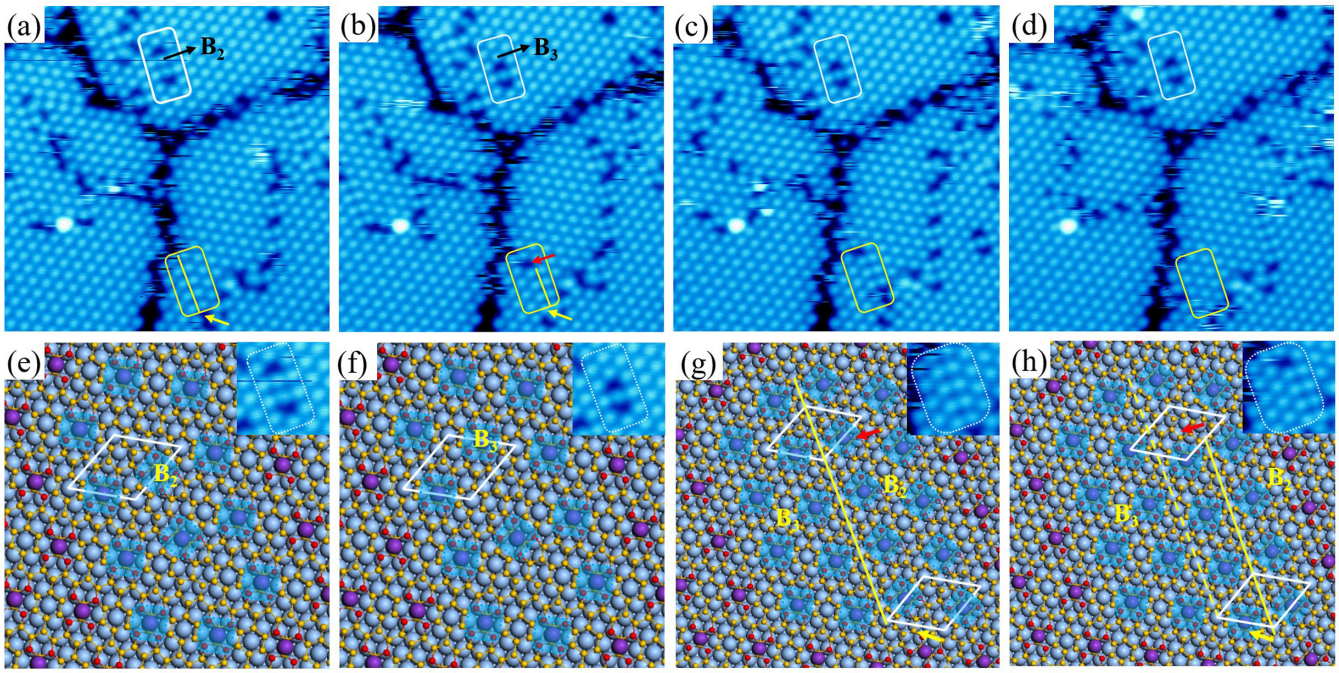

FIG. 5. The hopping of K atoms around vacancy defects and domain boundaries. (a–d) The sequential STM images show the movements of a vacancy defect (white rectangle) and an intradomain boundary (yellow rectangle). (e), (f) The structural models and the inset STM images show that one K atom changes its adsorption site from B_2 (e) to B_3 (f). (g), (h) The structural models and the inset STM images show that an intra-domain boundary moves from left to right (marked by the yellow line). The blue shaded areas represent K protrusions in the STM image. The white rhombuses are unit cells of the ordered K layer.

C. V-shaped density of states

Besides looking at the structural properties discussed above, we also performed scanning tunneling spectroscopy (STS) measurements on both clean silicene-(3 × 3) and the ordered K/silicene-(3 × 3) at 77 K to study the electronic properties. The black curve in Fig. 6(a) shows metallic density of states (DOS) in silicene-(3 × 3). As we know, silicene is predicted to be a two-dimensional Dirac material [5], and the Dirac cones in silicene-(3 × 3) had been reported by ARPES [4]. However, due to the strong coupling between silicene and the Ag(111) substrate [36], few reports of obvious Dirac features have been made in STS measurements. Upon K adsorption, we achieved an STS curve [the red curve in Fig. 6(a)] with a dip feature at about −0.1 V on ordered K/silicene-(3 × 3). The zoomed-in curve in Fig. 6(b) shows a nearly V-shaped density of states in the bias range of −0.35 to 0.20 V, which is one of the hallmarks of a two-dimensional Dirac material [37].

To qualitatively explain where this V-shaped DOS comes from, we first calculated the distribution of charge density in K/silicene-(3 × 3) around the Fermi level, which is shown in Figs. 6(c) and 6(d). Most of the charge densities (yellow) are focused on the silicene layer, while there is a small part on the interface of the silicene and the first layer of the Ag(111) substrate. Additionally, both our calculations and Ref. [8] show that the total DOS basically coincides with the partial DOS of silicene, whereas the *s* states of K are nearly empty and lie rather far above E_F, indicating that the observed V-shaped DOS near E_F originates from the contribution of the silicene layer.

We have also calculated the electronic band structure of silicene-(3 × 3)/Ag(111) before and after K adsorption based on the DFT calculations, which is further processed by the orbital-selective band unfolding technique [38,39]. The effective band structures (EBSs) are unfolded to the first Brillouin zone of Ag-(1 × 1) [inset of Fig. 6(e)] and projected onto the silicene layer. In Fig. 6(e), along the *K*-*M*-*K*′ direction, the band structures of silicene-(3 × 3)/Ag(111) above E_F show linear dispersion with two band tops located at ∼0.2 eV above E_F. According to the work of Feng *et al.* [4], both of the two band tops correspond to a pair of Dirac points which derive from the original Dirac cone of freestanding silicene at *K* (*K*′) points that folded onto the *M* point of Ag-(1 × 1). They are split into pairs by periodic potentials that originate from the interaction between the Ag(111) substrate and the silicene-(3 × 3) overlayer. At the *M* point of Ag(111) in Fig. 6(e), the band bottom that located at ∼0.4 eV below E_F also agrees with the saddle point reported in previous ARPES results [4], which confirms again our energy band calculation. After K adsorption, the overall band structure in Fig. 6(f) does not change that much but shifts downward because of electron doping from K to silicene-(3 × 3)/Ag(111). It should be noted that the binding energy of the Dirac cone pairs moves from ∼0.2 eV above E_F to ∼0.1 eV below E_F. In 2016, Feng *et al.* also observed the downward shifting of silicene Dirac cone pairs when increasing the doping amount of K atoms in ARPES measurements [40]. Since the location of the dip feature that appeared in the STS curve of K/silicene-(3 × 3) [Fig. 6(b)] coincides with the calculated band structure in Fig. 6(f), and the V-shaped DOS originates from the contribution of the silicene layer, we suppose that the dip corresponds to the Dirac point of silicene. The deposition of K atoms may change the interaction between silicene-(3 × 3) and the Ag(111) sub-

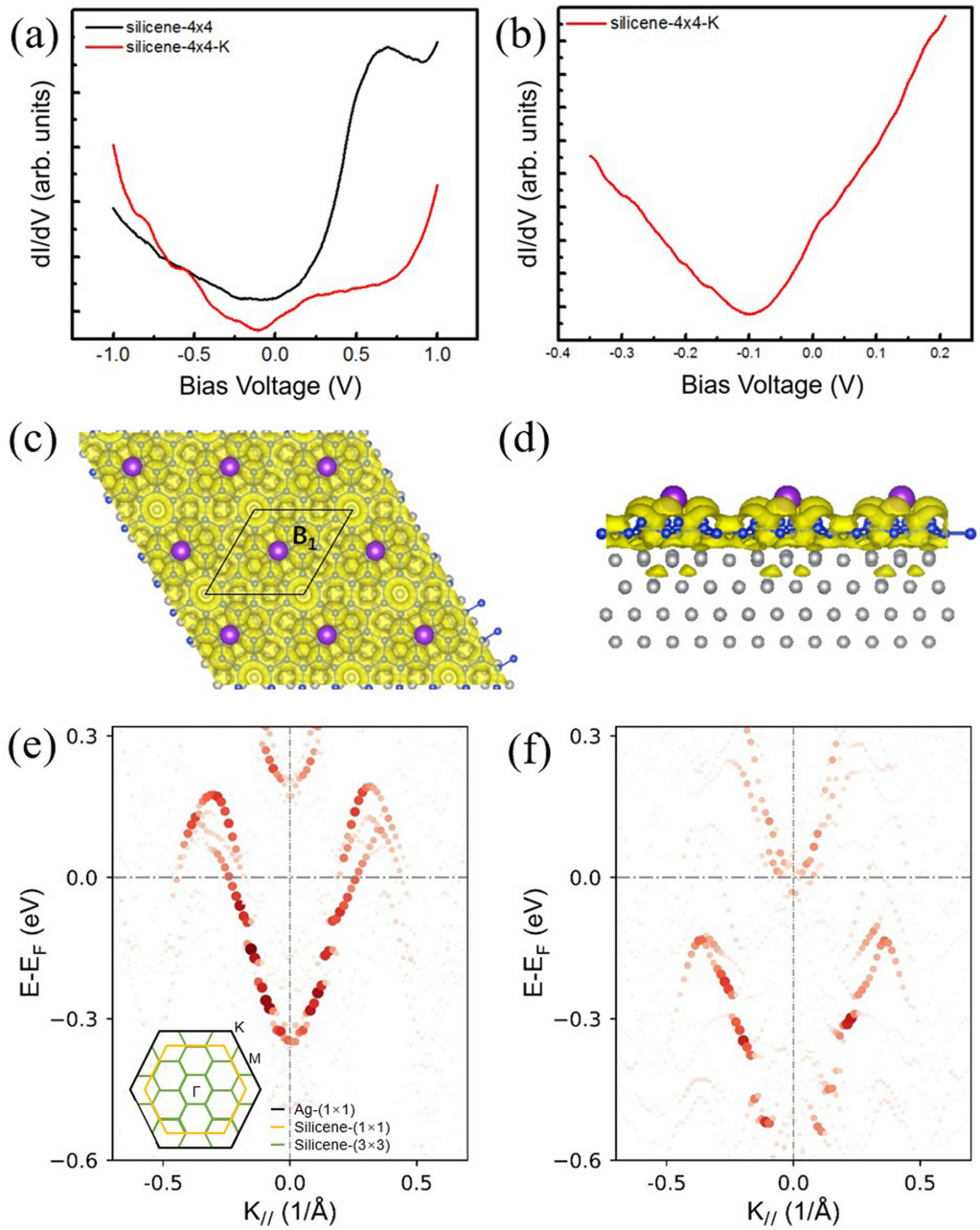

FIG. 6. The electronic properties of ordered K/silicene. (a) The STS curves of silicene-(3 × 3) (black curve) and ordered close-packed K/silicene-(3 × 3) (red curve). (b) The nearly V-shaped density of states of K/silicene around the Fermi level. (c,d) The top and side views of charge density distribution on ordered K/silicene around the Fermi level by DFT calculations. The charge density distribution is given by the local density of states integrated from 0.5 eV below the Fermi level to 0.5 eV above the Fermi level. The yellow color represents the charge densities, which are basically contributed from the silicene layer. (e) The effective band structure of the clean silicene-(3 × 3) along the high-symmetry path of *K*-*M*-*K*′. The size and color of the dots denote spectral weight. The vertical and horizontal dashed lines show the position of the Fermi surface and the position of the *M* point, respectively. The inset shows the Brillouin zones of the silicene-(1 × 1) (yellow lines), the Ag-(1 × 1) (black lines), and the silicene-(3 × 3) superstructure (green lines). (f) The effective band structure of the ordered close-packed K/silicene-(3 × 3). Upon K adsorption, the two Weyl points shift to ∼0.1 eV below the Fermi surface.

strate, so we can therefore detect the Dirac signature of silicene in STS measurement. However, to explain quantitatively the interface interaction details in the K/silicene-(3 × 3)/Ag(111) system, further experiments and calculations are still needed.

IV. CONCLUSION

In summary, we reveal the structural and electronic properties of K on silicene-(3 × 3)/Ag(111) by LT-STM and DFT. A phase transition from a dispersed phase to an ordered close-packed K layer has been demonstrated with the increasing

of K coverages. In the dispersed phase, K atoms selectively adsorb on silicene-(3×3) in low K coverages. In the ordered phase, three K adsorption sites have been calculated by DFT, agreeing well with the STM observations. STS measurements show a nearly V-shaped DOS on the ordered K/silicene-(3×3), which is supposed to be the Dirac signature of silicene-(3×3) by the electronic band calculations. Our work provides a comprehensive picture for K on silicene-(3×3) and a realistic pathway for future studies of AM atoms on other two-dimensional graphenelike materials.

ACKNOWLEDGMENTS

We thank B. Feng and W. Wang for valuable discussions. This work was supported by the National Natural Science Foundation of China (Grants No. 11604075 and No. 12174084), the Natural Science Foundation of Hebei Province (Grants No. A2017205122 and No. A2021205024), and China Postdoctoral Science Foundation (Grants No. BX201700068 and No. 2017M620095).

C.W. and H.W. contributed equally to this work.

[1] K. Takeda and K. Shiraishi, Theoretical possibility of stage corrugation in Si and Ge analogs of graphite, Phys. Rev. B **50**, 14916 (1994).

[2] G. G. Guzmán-Verri and L. C. Lew Yan Voon, Electronic structure of silicon-based nanostructures, Phys. Rev. B **76**, 075131 (2007).

[3] C. C. Liu, W. Feng, and Y. Yao, Quantum Spin Hall Effect in Silicene and Two-Dimensional Germanium, Phys. Rev. Lett. **107**, 076802 (2011).

[4] B. Feng, H. Zhou, Y. Feng, H. Liu, S. He, I. Matsuda, L. Chen, E. F. Schwier, K. Shimada, S. Meng, and K. Wu, Superstructure-Induced Splitting of Dirac Cones in Silicene, Phys. Rev. Lett. **122**, 196801 (2019).

[5] S. Cahangirov, M. Topsakal, E. Akturk, H. Sahin, and S. Ciraci, Two- and One-Dimensional Honeycomb Structures of Silicon and Germanium, Phys. Rev. Lett. **102**, 236804 (2009).

[6] N. D. Drummond, V. Zolyomi, and V. I. Fal'ko, Electrically tunable band gap in silicene, Phys. Rev. B **85**, 075423 (2012).

[7] Y. Fukaya, I. Mochizuki, M. Maekawa, K. Wada, T. Hyodo, I. Matsuda, and A. Kawasuso, Structure of silicene on a Ag(111) surface studied by reflection high-energy positron diffraction, Phys. Rev. B **88**, 205413 (2013).

[8] X. Lin and J. Ni, Much stronger binding of metal adatoms to silicene than to graphene: A first-principles study, Phys. Rev. B **86**, 075440 (2012).

[9] R. Quhe, R. Fei, Q. Liu, J. Zheng, H. Li, C. Xu, Z. Ni, Y. Wang, D. Yu, Z. Gao, and J. Lu, Tunable and sizable band gap in silicene by surface adsorption, Sci. Rep. **2**, 853 (2012).

[10] H. Sahin and F. M. Peeters, Adsorption of alkali, alkaline-earth, and 3*d* transition metal atoms on silicene, Phys. Rev. B **87**, 085423 (2013).

[11] J. Sivek, H. Sahin, B. Partoens, and F. M. Peeters, Adsorption and absorption of boron, nitrogen, aluminum, and phosphorus on silicene: Stability and electronic and phonon properties, Phys. Rev. B **87**, 085444 (2013).

[12] J. J. Zhao, H. S. Liu, Z. M. Yu, R. G. Quhe, S. Zhou, Y. Y. Wang, C. C. Liu, H. X. Zhong, N. N. Han, J. Lu, Y. G. Yao, and K. H. Wu, Rise of silicene: A competitive 2D material, Prog. Mater. Sci. **83**, 24 (2016).

[13] Y. Du, J. Zhuang, H. Liu, X. Xu, S. Eilers, K. Wu, P. Cheng, J. Zhao, X. Pi, K. W. See, G. Peleckis, X. Wang, and S. X. Dou, Tuning the band gap in silicene by oxidation, ACS Nano **8**, 10019 (2014).

[14] Y. Du, J. Zhuang, J. Wang, Z. Li, H. Liu, J. Zhao, X. Xu, H. Feng, L. Chen, K. Wu, X. Wang, and S. X. Dou, Quasi-freestanding epitaxial silicene on Ag(111) by oxygen intercalation, Sci. Adv. **2**, e1600067 (2016).

[15] J. Qiu, H. Fu, Y. Xu, A. I. Oreshkin, T. Shao, H. Li, S. Meng, L. Chen, and K. Wu, Ordered and Reversible Hydrogenation of Silicene, Phys. Rev. Lett. **114**, 126101 (2015).

[16] J. Qiu, H. Fu, Y. Xu, Q. Zhou, S. Meng, H. Li, L. Chen, and K. Wu, From silicene to half-silicane by hydrogenation, ACS Nano **9**, 11192 (2015).

[17] D. B. Medina, E. Salomon, G. Le Lay, and T. Angot, Hydrogenation of silicene films grown on Ag(111), J. Electron Spectrosc. Relat. Phenomen. **219**, 57 (2017).

[18] M. Caragiu and S. Finberg, Alkali metal adsorption on graphite: A review, J. Phys.: Condens. Matter **17**, R995 (2005).

[19] F. Yin, J. Akola, P. Koskinen, M. Manninen, and R. E. Palmer, Bright Beaches of Nanoscale Potassium Islands on Graphite in STM Imaging, Phys. Rev. Lett. **102**, 106102 (2009).

[20] E. Olsson, G. Chai, M. Dove, and Q. Cai, Adsorption and migration of alkali metals (Li, Na, and K) on pristine and defective graphene surfaces, Nanoscale **11**, 5274 (2019).

[21] K. T. Chan, J. B. Neaton, and M. L. Cohen, First-principles study of metal adatom adsorption on graphene, Phys. Rev. B **77**, 235430 (2008).

[22] K. Wu, Unusual diffusivity and clustering of alkali metals on the Si(111)-7 × 7 surface, Sci. Technol. Adv. Mater. **6**, 789 (2005).

[23] H. Zheng and R. E. Palmer, Bias-dependent scanning tunneling microscopy investigation of potassium adsorption on a Si(111)-7 × 7 surface, Phys. Rev. B **80**, 073304 (2009).

[24] J. Wang, J. B. Li, S. S. Li, and Y. Liu, Hydrogen storage by metalized silicene and silicane, J. Appl. Phys. **114**, 124309 (2013).

[25] T. Hussain, S. Chakraborty, and R. Ahuja, Metal-functionalized silicene for efficient hydrogen storage, ChemPhysChem **14**, 3463 (2013).

[26] R. Friedlein, A. Fleurence, J. T. Sadowski, and Y. Yamada-Takamura, Tuning of silicene-substrate interactions with potassium adsorption, Appl. Phys. Lett. **102**, 221603 (2013).

[27] G. Kresse and J. Furthmüller, Efficient iterative schemes for *ab initio* total-energy calculations using a plane-wave basis set, Phys. Rev. B **54**, 11169 (1996).

[28] J. P. Perdew, K. Burke, and M. Ernzerhof, Generalized Gradient Approximation Made Simple, Phys. Rev. Lett. **77**, 3865 (1996).

[29] H. Jamgotchian, Y. Colignon, N. Hamzaoui, B. Ealet, J. Y. Hoarau, B. Aufray, and J. P. Bibérian, Growth of silicene layers on Ag(111): Unexpected effect of the substrate temperature, J. Phys.: Condens. Matter **24**, 172001 (2012).

[30] B. Feng, Z. Ding, S. Meng, Y. Yao, X. He, P. Cheng, L. Chen, and K. Wu, Evidence of silicene in honeycomb structures of silicon on Ag(111), Nano Lett. **12**, 3507 (2012).

[31] H. Enriquez, S. Vizzini, A. Kara, B. Lalmi, and H. Oughaddou, Silicene structures on silver surfaces, J. Phys.: Condens. Matter **24**, 314211 (2012).

[32] P. Moras, T. O. Mentes, P. M. Sheverdyaeva, A. Locatelli, and C. Carbone, Coexistence of multiple silicene phases in silicon grown on Ag(111), J. Phys.: Condens. Matter **26**, 185001 (2014).

[33] Z. Y. Li, K. M. Hock, and R. E. Palmer, Phase Transitions and Excitation Spectrum of Submonolayer Potassium on Graphite, Phys. Rev. Lett. **67**, 1562 (1991).

[34] K. Wu, Y. Fujikawa, T. Nagao, Y. Hasegawa, K. S. Nakayama, Q. K. Xue, E. G. Wang, T. Briere, V. Kumar, Y. Kawazoe, S. B. Zhang, and T. Sakurai, Na Adsorption on the Si(111)-(7 $\times$ 7) Surface: From Two-Dimensional Gas to Nanocluster Array, Phys. Rev. Lett. **91**, 126101 (2003).

[35] Z. L. Liu, M. X. Wang, J. P. Xu, J. F. Ge, G. Le Lay, P. Vogt, D. Qian, C. L. Gao, C. H. Liu, and J. F. Jia, Various atomic structures of monolayer silicene fabricated on Ag(111), New J. Phys. **16**, 075006 (2014).

[36] Y. K. Yuan, R. G. Quhe, J. X. Zheng, Y. Y. Wang, Z. Y. Ni, J. J. Shi, and J. Lu, Strong band hybridization between silicene and Ag(111) substrate, Physica E **58**, 38 (2014).

[37] Z. Qin, J. Pan, S. Lu, Y. Shao, Y. Wang, S. Du, H. J. Gao, and G. Cao, Direct evidence of Dirac signature in bilayer germanene islands on Cu(111), Adv. Mater. **29**, 1606046 (2017).

[38] P. V. C. Medeiros, S. Stafström, and J. Björk, Effects of extrinsic and intrinsic perturbations on the electronic structure of graphene: Retaining an effective primitive cell band structure by band unfolding, Phys. Rev. B **89**, 041407(R) (2014).

[39] P. V. C. Medeiros, S. S. Tsirkin, S. Stafström, and J. Björk, Unfolding spinor wave functions and expectation values of general operators: Introducing the unfolding-density operator, Phys. Rev. B **91**, 041116(R) (2015).

[40] Y. Feng, D. Liu, B. Feng, X. Liu, L. Zhao, Z. Xie, Y. Liu, A. Liang, C. Hu, Y. Hu, S. He, G. Liu, J. Zhang, C. Chen, Z. Xu, L. Chen, K. Wu, Y.-T. Liu, H. Lin, Z.-Q. Huang *et al.*, Direct evidence of interaction-induced Dirac cones in a monolayer silicene/Ag(111) system, Proc. Natl. Acad. Sci. U. S. A. **113**, 14656 (2016).